Mean-field behavior of cluster dynamics

N. Persky*
Racah Institute of Physics, Hebrew University, Jerusalem 91904, Israel

R. Ben-Av† and I. Kanter‡
Department of Physics, Bar-Ilan University, Ramat-Gan 52100, Israel

E. Domany§
Department of Physics of Complex Systems, Weizmann Institute of Science, Rehovot 76100, Israel
(Received 19 March 1996)

The dynamic behavior of cluster algorithms is analyzed in the classical mean-field limit. Rigorous analytical results below T_c establish that the dynamic exponent has the value $z_{SW}=1$ for the Swendsen-Wang algorithm and $z_W=0$ for the Wolff algorithm. An efficient Monte Carlo implementation is introduced, adapted for using these algorithms for fully connected graphs. Extensive simulations both above and below T_c demonstrate scaling and evaluate the finite-size scaling function by means of a rather impressive collapse of the data. [S1063-651X(96)09608-0]

PACS number(s): 05.50.+q, 75.40.Mg, 64.60.Ht

I. INTRODUCTION

In a series of seminal pioneering papers Fortuin and Kasteleyn [1] established an important connection between percolation problems and the related concept of clusters, on the one hand, and various thermodynamic functions of Potts spin models, on the other. These connections allow geometric interpretation of different properties of these systems that play a central role in their critical behavior. For example, the onset of spontaneous magnetization coincides with the appearance of an infinite cluster in the related percolation problem; the susceptibility is proportional to the mean cluster size and the correlation length to a typical cluster's radius.

Some years later Swendsen and Wang [2] used these ideas in a way that constituted a breakthrough in a different subfield of statistical physics: that of computer simulations of systems in thermal equilibrium. They exploited the Fourtuin-Kasteleyn mapping to define a very efficient Monte Carlo algorithm that performs large-scale nonlocal moves by flipping simultaneously entire clusters of spins. This dynamics decreases the relaxation time to equilibrium while preserving detailed balance and ergodicity. In this way one can overcome (or at least significantly reduce) critical slowing down at second-order phase transitions [3]. ''Critical slowing down'' is a well-known phenomenon; the relaxation time of a system diverges as the critical point is approached. The manifestation of this *real, physical* effect on simulations is that at criticality the typical time needed to produce a large set of decorrelated configurations, which appear with the proper Boltzmann weight, diverges with the system's size. Hence the standard local Metropolis-type Monte Carlo simulation methods become inefficient.

A wide variety of cluster methods have been applied successfully to many fields in physics (second-order phase transitions, disordered and frustrated systems, quantum field theories, fermions in a gauge background, quantum gravity, and more [4–11]). In many cases a dramatic acceleration of convergence to equilibrium was achieved. That is, if the simulation of a system of (linear) size L is performed at the critical point, the relaxation time behaves according to $\tau \sim L^{z_c}$ where z_c, the exponent associated with the cluster algorithm is significantly less than z_{local} of the local methods.

So far only relatively few rigorous results have been derived for cluster algorithms and the associated relaxation times and exponents [4,6]. In this paper we consider the well-known version of the Ising spin model for which the mean field is the exact solution, that of $N \to \infty$ spins, all connected to each other. By analyzing this system one can calculate the classical, mean-field value of z_c.

The mean-field Ising ferromagnet has been previously examined analytically and numerically by Ray, Tamayo, and Klein (RTK) [4]. Although the work presented here agrees with the conclusions of RTK regarding the Swendsen-Wang (SW) dynamics, it contains some improvement. First, the derivation of the analytical results is improved by employing the known exact results of Erdös and Renyi [12] for highly diluted random graphs instead of the approximation (used by RTK) of a Bethe lattice with large coordination number. We show that this technical improvement does not alter the results obtained [4] for SW dynamics. Second, we performed simulations, introducing an efficient algorithm, that extend those of RTK in the following aspects. RTK looked at the relaxation times τ of the magnetization autocorrelation function, measured at a single temperature (T_c of the infinite system) versus the size of the system. In addition, they also studied the temperature dependence of τ below T_c at a single value of the system size. Our simulations were done on larger systems using longer running times; in addition, we studied a wide range of system sizes and temperatures both above and below T_c. Our analysis of the results is based on

*Electronic address: nathanp@vms.huji.ac.il
†Electronic address: radi@opal.co.il
‡Electronic address: ido@kanter.ph.biu.ac.il
§Electronic address: eytan@elect1.weizmann.ac.il

finite-size scaling; the relaxation times measured at various temperatures and system sizes are presented using data collapse, thereby also calculating numerically the corresponding finite-size scaling function. This data collapse of course takes into account the shift in the transition temperature as a function of the size of the system. It resolves the unexpected result that RTK found puzzling, namely, that the slowing down below the transition appeared to be enhanced in comparison to that at the transition. When the shift in the transition temperature is properly accounted for, this effect disappears.

In addition, we present analytical and numerical results for Wolff [11] dynamics with the conclusion that the relaxation times of the autocorrelation function depends on the details of the global algorithm. However, the upper critical dimension is hypothesized to be unaffected by the details of the local or the global algorithm.

II. MODEL

The Hamiltonian of the fully connected Ising model is defined by

$$\mathcal{H}=-\frac{1}{2N}\sum_{i\neq j=1}^{N} S_iS_j, \quad S_i=\pm 1. \tag{1}$$

The statics of this model is solved exactly, using a mean field [13]. The result is a second-order phase transition at $\beta_c=1$, with exponents $\alpha=0$, $\nu=0.5$, $\beta=0.5$, and $\gamma=1$. The local (single spin flip) dynamics of this model can also be solved exactly using a mean-field approach resulting in (from here we use $\beta=1/kT$ unless otherwise stated)

$$\tau(\beta)\propto(\beta-\beta_c)^{-1}.$$

Using the fact that $\nu=0.5$ [i.e., $\xi\propto(\beta-\beta_c)^{-1/2}$], it is clear that $\tau\propto\xi^2$, giving

$$z_{\rm local}=2.$$

The standard SW procedure as implemented for this model is defined as follows. Let us assume that the system is in a spin configuration $\{S_i\}$, $i=1,\ldots,N$. In each SW sweep every bond is ''activated'' (or frozen) with probability

$$P_f=1-\exp\left(-\frac{\beta}{N}(1+S_iS_j)\right). \tag{2}$$

A bond that is not frozen is called ''deleted.'' Frozen bonds define connected clusters, to each of which a spin value (± 1) is now assigned randomly, giving rise to the new spin configuration. Then the procedure is repeated. The dynamics of this SW procedure was studied for the fully connected model by Ray, Tamaya, and Klein [4], who showed that $z_{\rm SW}=1$.

We present now a different derivation of this result: one which utilizes exact results from graph theory. In order to get better insight into the percolation properties of the fully connected model let us introduce a few previously known facts about highly diluted graphs [12]. These are relevant to our problem since for $N\gg 1$ the freezing probability P_f is very small and the SW procedure generates precisely the highly diluted graphs to which we now turn.

Consider a graph of N nodes; on all links connecting pairs of nodes i,j place independent random variables J_{ij}, taken from the probability distribution

$$P(J_{ij})=(1-c/N)\,\delta(J_{ij})+(c/N)\,\delta(J_{ij}-1), \tag{3}$$

where the average connectivity c is taken to be $O(1)$. The resulting highly diluted graph has finite connectivity; in the thermodynamic limit the probability that a node has connectivity k (i.e., has nonvanishing link variables J_{ij} with k other nodes) follows the Poisson distribution

$$P(k)=c^k\exp(-c)/k!.$$

Many geometric properties of this diluted graph are well understood [12,14,15]. In particular, the graph undergoes a percolation transition at $c=1$. That is, the number of nodes that belong to the largest connected cluster is of $O(\log N)$ for $c<1$, $O(N^{2/3})$ at $c=1$, and $O(N)$ for $c>1$. In this percolating regime the size of the largest cluster is gN, where the parameter g is the solution of the equation [14]

$$g=1-e^{-cg}$$

or

$$\ln(1-g)=cg.$$

Assuming that for $c=1+\delta$ and $\delta\ll 1$ one has $g\ll 1$, we get

$$cg-g-g^2/2-g^3/3=0$$

and therefore

$$2g^2+3g-6\delta=0,$$

which yields

$$g(1+\delta)=2\delta-\tfrac{8}{3}\delta^2. \tag{4}$$

After this aside on random dilute graphs we return to the SW dynamics for our fully connected Ising spin model. Since the spins are fully connected, a configuration is fully parametrized by N_+, the number of positive valued spins, or by its magnetization

$$m=(N_+-N_-)/N,$$

where $N_-=N-N_+$. The dynamics is therefore completely characterized by specifying the value of either N_+ or m after each Monte Carlo sweep. Every SW sweep can be thought of as consisting of two steps. In the first step the spins are divided into two groups, one of positive spins (all the spins with $S_i=+1$) and the other negative (spins with $S_i=-1$). Using P_f of (2) we first note that all the links connecting any positive spin to any negative one are deleted. The positive (negative) group contains

$$N_\pm=\frac{N}{2}(1\pm m)$$

spins. Without loss of generality, we assume that $N_+ > N_-$.

In the second step, each group is examined independently. The internal links within a group are activated with the probability $P_f = 1 - \exp(-2\beta/N)$. Each group can be thought of now as a random graph with effective connectivity

$$c_\pm = P_f N_\pm \approx \frac{2\beta N_\pm}{N}. \tag{5}$$

Denoting by t the deviation from criticality, $\beta = 1 - t$ (recall that $\beta_c = 1$), we can write for the larger (positive) group of spins

$$c_+ = (1-t)(1+m). \tag{6}$$

We can now view the act of freezing a bond as choosing $J_{ij} = 1$ in the generation of the dilute graph discussed above. For that problem, as was mentioned previously, $c = 1$ is a critical value. Therefore, in the disordered phase of our spin model $t > 0$ and $\beta < \beta_c$ so that both $c_+, c_- < 1$ and the SW freeze-delete procedure creates only small (nonmacroscopic) clusters. On the other hand, at temperatures just below criticality, i.e., when $t < 0$, we have $c_+ > 1$ but $c_- < 1$. Hence only *one* macroscopic cluster (of positive spins), whose size is proportional to the lattice size, is generated, while the rest of the clusters are small.

Flipping of this single macroscopic cluster is the dominant element of the dynamics. The rest of the clusters are small—there are $O(N)$ of them—and therefore the extent that their flip influences the magnetization is negligible compared to that of the large cluster.

In what follows we derive recursion for N_+^l and m_l the values that the number of the majority spins and the magnetization take after l steps of the SW procedure. We use the notation N_+, but mean the number of spins in the state with majority (even when they are negative).

The small clusters become ± 1 with probability 1/2 after a sweep: neglecting fluctuations of their contribution and assuming that the single large spanning cluster was and remains positive, we can write

$$N_+^{l+1} = \tfrac{1}{2} N_-^l + \tfrac{1}{2}[N_+^l - N_+^l g(c_+)] + N_+^l g(c_+), \tag{7}$$

$$N_-^{l+1} = \tfrac{1}{2} N_-^l + \tfrac{1}{2}[N_+^l - N_+^l g(c_+)]. \tag{8}$$

Denoting $n_l = N_+^l/N$, Eqs. (7) and (8) can be rewritten as a recursion for the magnetization:

$$m_{l+1} = n_l g(2\beta n_l) = \frac{1+m_l}{2} g[(1-t)(1+m_l)]. \tag{9}$$

For simplicity we keep m positive (or, in other words, our recursion is actually for $|m|$).

Near the transition the argument of the function g is near its critical value and we can identify δ [see Eq. (4)] by

$$\delta = -t + m_l - t m_l.$$

Equation (4) is now given (up to terms of order $t^{3/2}$) by

$$m_{l+1} = \frac{1+m_l}{2}[2(-t + m_l - t m_l) - \tfrac{8}{3}(m_l^2 - t m_l)]$$

$$= m_l - t + \tfrac{2}{3} m_l t - \tfrac{1}{3} m_l^2, \tag{10}$$

which leads to the differential form

$$\frac{dm}{dl} = -t + \tfrac{2}{3} m_l t - \tfrac{1}{3} m_l^2 \tag{11}$$

where l, the discrete index of the sweep, has become a continuous ''time.'' For $t < 0$ Eq. (11) has a stationary point at

$$m^\star = (-3t)^{1/2}. \tag{12}$$

Near this point we write

$$m = m^\star + \epsilon$$

and linearize Eq. (11) in ϵ:

$$\frac{d\epsilon}{dl} = \tfrac{2}{3}\epsilon t - \tfrac{2}{3} m_l^\star \epsilon = \tfrac{2}{3}\epsilon t - \frac{2}{\sqrt{3}}\epsilon(-t)^{1/2}. \tag{13}$$

For $|t| \ll 1$ the $(-t)^{1/2}$ term is dominant so one can conclude that relaxation is dominated by

$$\epsilon \propto \exp\left[-l \Big/ \left(\frac{2}{\sqrt{3}}(-t)^{1/2}\right)\right],$$

and therefore in the ordered phase we find the relaxation time

$$\tau^{\mathrm{SW}} = \frac{\sqrt{3}}{2}(-t)^{-1/2}. \tag{14}$$

Using the definition

$$\tau = (-t)^{-\nu z}$$

yields our result for the mean-field value of the dynamic exponent of the Swendsen-Wang procedure

$$z_{\mathrm{SW}} = 1.$$

III. NUMERICAL RESULTS

A. Algorithm

The standard version [2] of the SW algorithm visits, during a single sweep, each bond once and takes a freeze or delete decision [16]. The fully connected system [Eq. (1)] contains N spins and $N(N-1)/2$ links; consequently the usual SW algorithm requires $O(N^2)$ operations for one sweep of the system. For our choice of P_f [Eq. (2)], however, only a very small fraction of bonds is eventually frozen: even though every spin has $O(N)$ links, only $O(1)$ are activated. Moreover, as explained in the Introduction, in the fully connected model the only relevant parameter that determines the system's state is its magnetization, or N_+. Hence, to get the new configuration *after* the SW sweep, all we have to determine is the new value of N_+. To do this we do not have to scan all $O(N)$ bonds of a certain spin; rather, when the algorithm ''visits'' a new spin that belongs to a cluster, it suffices to use the binomial distribution to deter-

mine the number of activated bonds it has (i.e., the number of new members of the cluster).

Therefore the SW algorithm can be implemented for the fully connected model by manipulating a few *numbers*, instead of the values taken by the spins. This approach simplifies the algorithm, is much more efficient, and uses a very small memory.

We adopted the spirit of the Wolff algorithm to grow all SW clusters during a sweep. At a given moment we know the number of spins that have been assigned to our presently growing cluster. New spins that have been added to the cluster have to be tested for the number of frozen bonds connecting them to *free* spins (that do not yet belong to any cluster and have the same sign as the presently growing cluster and hence are candidates for joining it). The spins that are known to belong to the cluster but have not yet been tested are in a ''*stack.*'' As a cluster is growing, the algorithm tracks and modifies the following parameters: N_c, the number of spins in the growing cluster; N_s the number of spin in the stack; and N_f the number of ''free spins.'' A SW sweep starts at a configuration with N_+ ''up'' spins and N_- ''down'' spins. Say we start to generate clusters of the up spins. The following steps are taken.

(i) Assign one spin to the growing cluster: set $N_c=N_s=1$ and $N_f=N_+-1$.

(ii) Test the spin: that is, using the binomial distribution, determine N_{add}, the number of frozen links our spin will get, connecting it to presently free spins:

$$\mathrm{Prob}(N_{\mathrm{add}})=\begin{pmatrix} N_f \\ N_{\mathrm{add}} \end{pmatrix} P_f^{N_{\mathrm{add}}}(1-P_f)^{N_f-N_{\mathrm{add}}}. \tag{15}$$

(iii) Update
$N_c=N_c+N_{\mathrm{add}}$,
$N_s=N_s+N_{\mathrm{add}}-1$,
$N_f=N_f-N_{\mathrm{add}}$.

(iv) Perform another test (as long as $N_s>0$) using step (ii). Repeat (ii)–(iv) until the stack is empty ($N_s=0$). Construction of the cluster has now been completed.

(v) Flip the cluster with probability $\frac{1}{2}$. If the cluster has flipped, the value of the magnetization changes:

$$M\rightarrow M-2N_c.$$

(vi) Reset $N_c=1$, $N_s=1$, and $N_f=N_f-1$ and repeat (ii)–(vi) to construct new clusters, until there are no more free spins ($N_f=0$).

(vii) Go to the second component (of down spins) and apply (i)–(vi) with N_-. Note that now when the cluster flips the magnetization *increases* by $2N_c$.

Note that all the operations of our algorithm are on a few *numbers*, namely, we do not really define spins, just manipulate a few counters that were defined above. For the Wolff version one can apply the same algorithm and grow only the first cluster; the decision of starting it from an up or down spin as seed is done at random (with probability proportional to the number of up or down spins).

B. Finite-size scaling analysis

Finite-size scaling is a standard method [17,18] to extract critical indices from numerical data obtained by simulating finite systems of linear size L. Denote by t the reduced temperature variable and by $\mathcal{B}$ a thermodynamic quantity that exhibits singular behavior in the $L\rightarrow\infty$ limit, characterized by the exponent θ:

$$\mathcal{B}\propto t^{-\theta}. \tag{16}$$

For a finite system clearly $\mathcal{B}$ is an analytic function of t and the finite-size scaling function exhibits a crossover; when t is such that the correlation length $\xi\sim t^{-\nu}$ is much smaller than the system size L the function behaves like (16); in the $L\rightarrow\infty$ limit all dependence on L should disappear. On the other hand, for $\xi\leqslant L$ the finite-size effects wipe the singularity out.

The scaling hypothesis [17] asserts that the crossover scaling function depends on L only through the ratio L/ξ and one expects the form

$$\mathcal{B}(t,L)=L^{\theta/\nu}f(L/\xi)=\xi^{\theta/\nu}g(L/\xi). \tag{17}$$

This scaling form includes implicitly the finite-size shift of $T_c(L)$, which is defined by the temperature at which the measured quantity has a peak. The size of this shift generally has the form

$$|T_c(L)-T_c(\infty)|\propto L^{1/\nu}. \tag{18}$$

The specific scaling functions that we consider in this paper are, for the susceptibility,

$$\chi(t,L)=L^{\gamma/\nu}f(tL^{1/\nu}) \tag{19}$$

and, for the relaxation time,

$$\tau(t,L)=L^{z}f(tL^{1/\nu}). \tag{20}$$

C. Details of the simulations

The Monte Carlo simulations were carried out with the algorithm described above, for systems that contain $N=10^4-(3\times10^5)$ spins. The number of Monte Carlo sweeps per spin was 10^5. The first 10^4 configurations of the simulation (at list 500 times the relaxation time itself) were discarded in order to ensure that the system reached equilibrium.

The static equilibrium property that we measured was

$$\chi'=\beta N(\langle m^2\rangle-\langle|m|\rangle^2), \tag{21}$$

which is proportional to the ''real'' susceptibility χ [7]. The reason for this choice is that in finite systems, especially with cluster dynamics, the quantity $\langle m^2\rangle-\langle m\rangle^2$ has no peak at all and the measured value increases monotonically as T decreases. The reason is that m changes sign frequently and therefore $\langle m\rangle\sim0$. The method that determines χ by measuring the size of the SW clusters [11] also yields no peak.

To demonstrate the quality of our numerical data we present in Fig. 1 the susceptibility χ, as obtained from simulations and exact evaluation for a system of $N=20\,000$ spins. The exact result was derived by calculating $\langle m^2\rangle$ and $\langle|m|\rangle$ in (21), using the analytic expressions for the Boltzmann and entropic weights of all configurations with N_+ up spins (and summing over N_+).

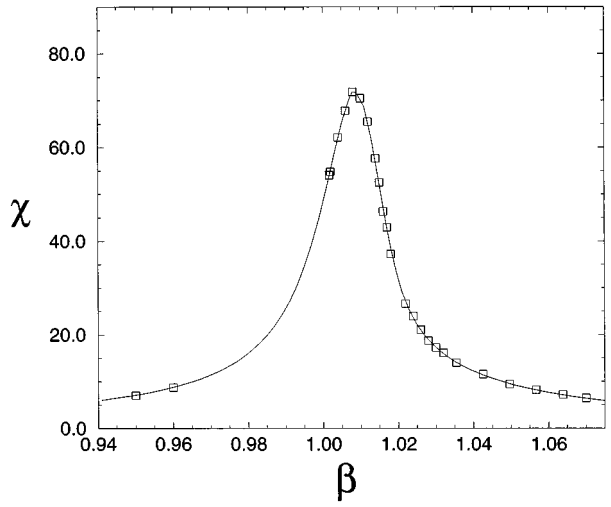

FIG. 1. Susceptibility χ vs β for a system of $N=20\,000$ spins. The solid line and squares represent exact results and the values obtained by simulations, respectively.

Figure 2 shows the susceptibility for different system sizes L as a function of temperature. One can see the large shift of the peak position for different sizes of the system.

The most striking manifestation of scaling is *data collapse*. The product $\chi L^{-\gamma/\nu}$ should depend only on $L/\xi \approx L\sqrt{\Delta\beta}$, where $\Delta\beta=\beta-1$. This can be seen very clearly in Fig. 3, where the mean-field exponents $\gamma/\nu=2$ and $\nu=1/2$ were used [we plotted the scaling function versus $(L/\xi)^2$]. In addition to presenting the scaling function and verification of the scaling form, the excellent data collapse that can be seen verifies the accuracy of our numerical simulations. The shift of the effective $T_c(L)$ is studied in Fig. 4; indeed one can see that the size of the shift agrees very well with Eq. (18), with the theoretical mean field value $\nu=\frac{1}{2}$.

The dynamic property that we measured is the time-dependent correlation function of the absolute value of the magnetization. The measurements were taken after every sweep. We considered the normalized correlation function of the absolute value of the magnetization

$$\rho(t)=\frac{\langle|m(t')m(t'+t)|\rangle-\langle|m|\rangle^2}{\langle m^2\rangle-\langle|m|\rangle^2}, \tag{22}$$

for which the integrated relaxation time, defined by

$$\tau_{int}=\tfrac{1}{2}+\sum_{t=1}^{\infty}\rho(t), \tag{23}$$

was calculated.

Figure 5 shows τ for different sizes of the system at various temperatures. As in the case of the susceptibility, one can see the large shift of the peak of the scaling function for different system sizes. Figure 4 contains also the scaling analysis of this shift as a function of L: again, the result agrees very well with the theoretical prediction. Note that,

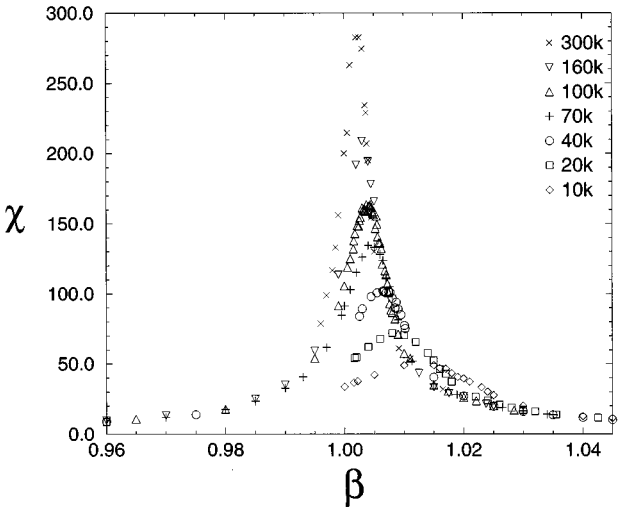

FIG. 2. Susceptibility χ versus β for different system sizes, measured in the vicinity of the bulk critical temperature $\beta_c=1$.

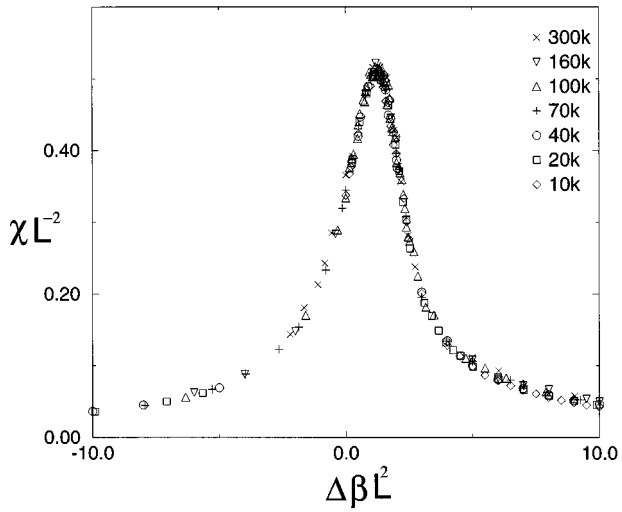

FIG. 3. Susceptibility scaling function [Eq. (19)]. The mean-field value of $\gamma/\nu=2$ was used for collapsing the data of Fig. 2.

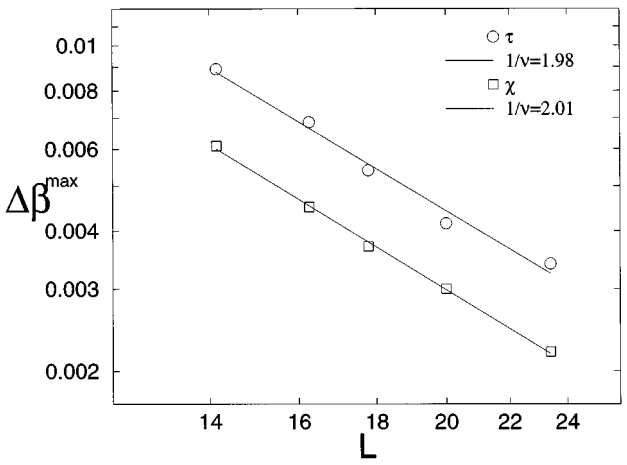

FIG. 4. Shift of the peak $\Delta\beta^{\max}=\beta^{\max}(L)-1$ of the susceptibility χ and of the integrated relaxation time τ plotted versus $L=N^{1/4}$. The nonlinear least-squares fit yielded the values $1/\nu=1.98\pm0.12$ for χ and $1/\nu=2.01\pm0.05$ for τ.

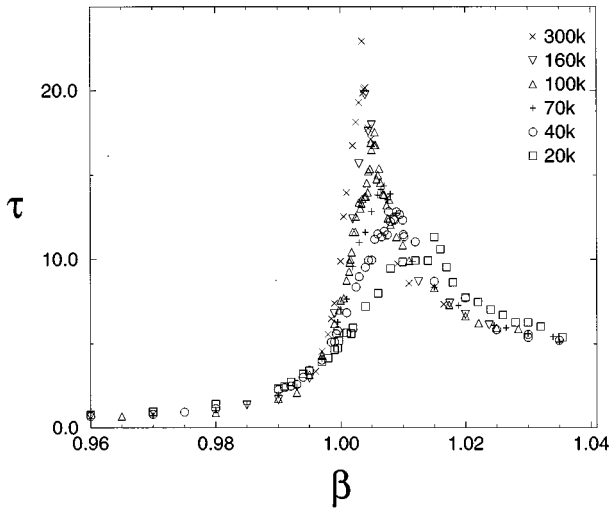

FIG. 5. Integrated relaxation time τ plotted versus β for different system sizes in the vicinity of the bulk critical temperature $\beta_c=1$.

although the slope is the same as in the susceptibility case, the shift is much larger, i.e., the amplitude is larger.

For reasonable sizes of the systems (such as the sizes that could be treated with computational power available to us) one cannot neglect this shift. For example, calculating τ (as well as any other quantity) for different system sizes *at* $T_c(\infty)(=1)$ and trying a fit of the form

$$\tau(T_c(\infty))=L^z$$

introduces some systematic errors.

Figure 6 presents the first measurement (to our knowledge) of a scaling function for τ. The theoretically derived value $z=1$ was used. The evident data collapse indicates a good fit to the scaling form presented in Eq. (20) and to the predicted z.

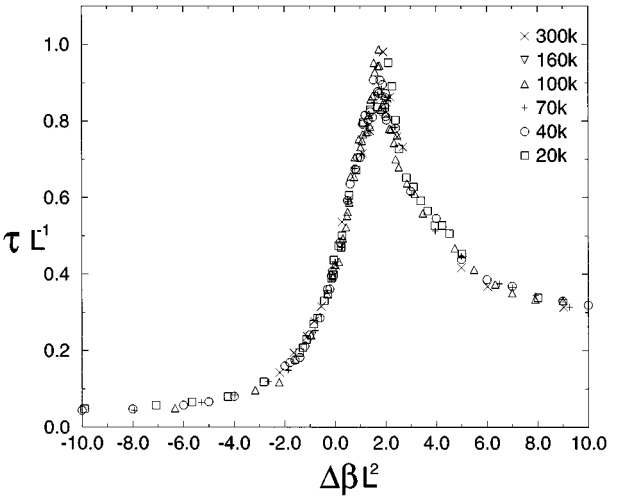

FIG. 6. Scaling function for the integrated relaxation time [Eq. (20)]. The value $z=1$ was used for collapsing the data of Fig. 5 .

IV. WOLFF DYNAMICS

Let us start with a remark about SW dynamics. Going back to Eq. (8) one can see that for a particular version of SW algorithm, in which one flips only the spanning cluster, the following equations are obtained:

$$N_+^{l+1}=N_+^l-N_+^l g(c_+), \tag{24}$$

$$N_-^{l+1}=N_-^l+N_+^l g(c_+). \tag{25}$$

Denoting N_+^l/N by n_l, this yields

$$\begin{aligned} m_{l+1}&=m_l-2n_l g(2\beta n_l)\\ &=m_l-(1+m_l)g[(1-t)(1+m_l)]. \end{aligned} \tag{26}$$

Keeping m positive, one would get instead of Eq. (11)

$$\frac{dm}{dl}=-2t+\tfrac{4}{3}m_l t-\tfrac{2}{3}m_l^2. \tag{27}$$

Going over the previous calculation [Eqs. (11)–(14)] one gets the same fixed point, the critical exponents do not change, and only a factor $\frac{1}{2}$ multiplies the prefactor in the expression for τ. That is,

$$\tau^{\mathrm{SW1}}=\tfrac{1}{2}\tau^{\mathrm{SW}}.$$

This result shows that flipping the spanning cluster constitutes the central component of the relaxation process. Moreover, it shows that flipping small clusters together with the flip of the spanning cluster does not help the relaxation at all.

We turn now to Wolff dynamics and calculate $\tau^W(\beta)$ in the thermodynamic limit, for $T>T_c$. We calculate τ^W in two steps. In the first step we calculate τ_c^W, the relaxation time measured using every single cluster update as one unit of time. In the second step, we normalize these Wolff time units to regular time units (N spins are accessed or updated in a single regular unit of time). To achieve this normalization we multiply the time measured in Wolff time units by the ratio of the average cluster size $\langle C\rangle$ to the system size N.

To calculate τ_c^W note that

$$\begin{aligned} \tau_c^W&=\tau^{\mathrm{SW1}}\frac{N}{\hat{C}}=\tfrac{1}{2}\tau^{\mathrm{SW}}\frac{N}{\hat{C}}\\ &=\tfrac{1}{2}\tau^{\mathrm{SW}}\frac{1}{g}\frac{N}{N_+}=\frac{\tau^{\mathrm{SW}}}{(1+m)g}\approx\frac{\tau^{\mathrm{SW}}}{g}, \end{aligned} \tag{28}$$

where $\hat{C}=gN$ is the size of the macroscopic cluster. To understand the leftmost equality note that every cluster update of the Wolff procedure has a chance of $\hat{C}/N$ to hit the macroscopic cluster. The rest of the cluster updates are irrelevant in the thermodynamics limit. When normalized to regular units of whole lattice update we get

$$\tau^W=\tau_c^W\frac{\langle C\rangle}{N}, \tag{29}$$

where $\langle C\rangle$ is the average cluster size in the Wolff procedure.

We turn now to calculate $\langle C\rangle$, using the theory of random graphs [12]. For the N_- part $c<1$ and the cluster size dis-

tribution has only ''small clusters'' with average cluster size $r_1=O(1)$. For the N_+ part $c>1$ and the cluster size distribution has two components. The first component is that of ''small clusters'' with average cluster size $r_2=O(1)$ and the second component is a single spanning cluster, whose size depends linearly upon N_+ with size $g(c_+)N_+$. Therefore

$$\frac{\langle C\rangle}{N}=\frac{1}{N}\left[\frac{N_-}{N}r_1+\frac{N_+}{N}\left\{\sum_{w=\text{cluster size}\in N_+}P(w)w\right\}\right]$$
$$\approx\frac{1}{N}\left[\frac{N_-}{N}r_1+\frac{N_+}{N}\{[1-g(c_+)]r_2+g(c_+)[g(c_+)N_+]\}\right].$$

In the limit $N\to\infty$, the first two terms vanish and the leading term is $(N_+/N)^2g^2$. Thus we arrive at

$$\frac{\langle C\rangle}{N}\approx\frac{(1+m)^2g^2}{4}\approx\frac{g^2}{4}. \tag{30}$$

Combining Eqs. (14), (28), and (29), we find that

$$\tau^W\approx\tau^{\mathrm{SW}}g(c_+)(1+m)/4=\tau^{\mathrm{SW}}g[(1-t)(1+m)](1+m)/4. \tag{31}$$

Using Eq. (4) we expand g to obtain

$$\tau^W\approx\tau^{\mathrm{SW}}2(-t+m-tm)(1+m)/4\approx\tau^{\mathrm{SW}}m/2$$
$$\approx\frac{\sqrt{3}}{2}(-t)^{-1/2}\sqrt{3}(-t)^{1/2}/2\approx 0.75=\text{const.} \tag{32}$$

Thus we have shown that τ^W does not depend on t and hence $z=0$ for $T<T_c$.

V. NUMERICAL RESULTS (WOLFF DYNAMICS)

The Monte Carlo simulations were carried out using the algorithm described in Sec. III, growing only the first cluster. Systems that contain $N=(2\times10^4)-(3\times10^5)$ spins were simulated. The number of cluster flips was 2×10^6 for each run. The first 10^5 configurations of each simulation were discarded in order to ensure equilibration. As in the SW case, the dynamical property measured was the correlation function of the absolute value of the time series of the magnetization. The measurements were done after every four cluster updates. From the correlation function we calculated the integrated relaxation time. Finally, we normalized by the average cluster size as was measured during the simulation.

Figure 7 shows τ for different sizes of the system at various temperatures. In order to get the scaling function we performed data collapse for τ with the theoretical value of $z=0$.

The results is shown in Fig. 8, in which one can see a very good agreement with the scaling form presented at Eq. (20). In addition, the asymptotic behavior is consistent with the result of Eq. (32), valid for $\beta>\beta_c$ and $L\gg1$.

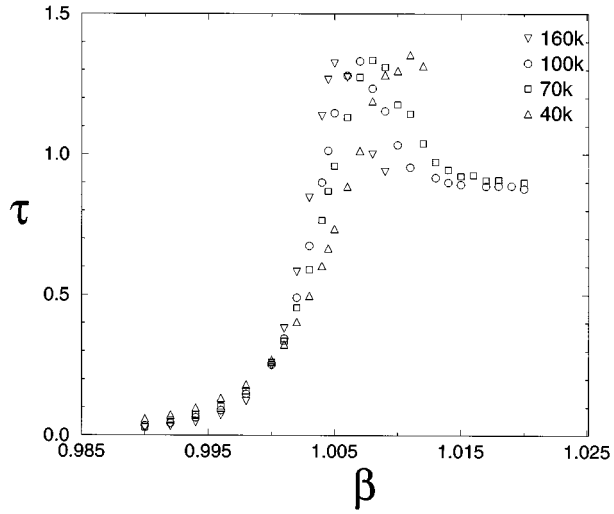

FIG. 7. Wolff integrated relaxation time τ^W plotted versus β for different system sizes in the vicinity of the bulk critical temperature $\beta_c=1$.

VI. SUMMARY AND CONCLUSIONS

Cluster algorithms constitute a significant advance in computational physics. Their associated dynamics is characterized by critical exponents that differ from those of standard methods. Very few exact results have so far been derived regarding these exponents.

In the present work we addressed the issue of the classical limit for the dynamic exponents of two cluster algorithms. For the Swendsen-Wang algorithm we found $z=1$; our analytical derivation of this result is based on rigorous results from the theory of random graphs. Since the proof applies only for the low-temperature phase, we measured the relaxation time τ^{SW}, using an implementation of the SW algorithm adapted for fully connected graphs, *both above and below* T_c. We established the scaling behavior of $\tau^{\mathrm{SW}}(t,L)$ by demonstrating rather conclusive data collapse. Previous

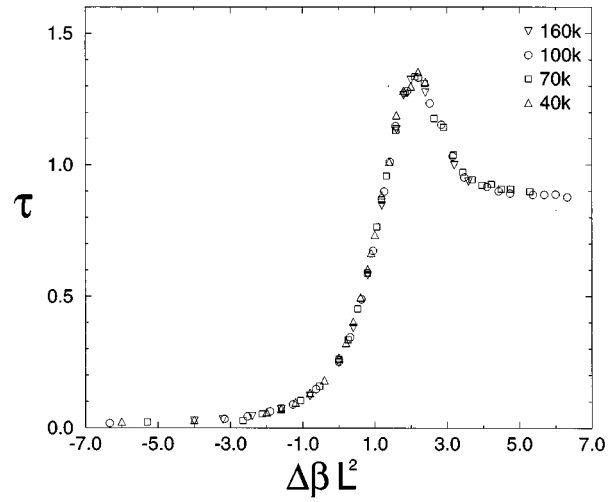

FIG. 8. Scaling function for the integrated relaxation time Eq. (20). The value $z=0$ was used for collapsing the data of Fig. 7.

work used a Bethe lattice approximation for the analytic derivation and did not present the full scaling function for the relaxation time.

For the single-cluster algorithm of Wolff we have shown that $z=0$ and presented numerical evidence, again obtained both above and below T_c. The scaling function was found numerically and data collapse was demonstrated.

ACKNOWLEDGEMENTS

We thank D. Kandel and S. Solomon for discussions and R. Swendsen for some illuminating comments and suggestions. This research was partially supported by grants from the U.S.–Israel BSF, the Germany-Israel Foundation, and the Israeli Academy of Sciences.

[1] C. M. Fortuin and P. W. Kasteleyn, Physica **57**, 536 (1972).
[2] R. H. Swendsen and J. S. Wang, Phys. Rev. Lett. **58**, 86 (1987).
[3] B. I. Halperin and P. C. Hohenberg, Rev. Mod. Phys. B **49**, 435 (1977).
[4] T. S. Ray, P. Tamayo, and W. Klein, Phys. Rev. A **39**, 5949 (1989).
[5] P. Tamayo, R. C. Brower, and W. Klein, J. Stat. Phys. **58**, 1083 (1990).
[6] X. J. Li and A. Sokal, Phys. Rev. Lett. **63**, 827 (1989)
[7] K. Binder and D. W. Herman, *Monte Carlo Simulation in Statistical Physics* (Springer-Verlag, Berlin, 1992).
[8] D. Kandel and E. Domany, Phys. Rev. B **43**, 8539 (1991).
[9] A. D. Sokal, in *Quantum Fields on The Computer*, edited by M. Creutz (World Scientific, Singapore, 1992), p. 211.
[10] S. Solomon, in *Annual Reviews of Computational Physics II*, edited by D. Stauffer (World Scientific, Singapore, 1995), pp. 243–294.
[11] U. Wolff, Phys. Rev. Lett. **62**, 361 (1989).
[12] P. Erdös and A. Renyi, in *The Art of Counting*, edited by J. Spencer (MIT Press, Cambridge, MA, 1973).
[13] R. Baxter, *Exactly Solved Models in Statistical Mechanics* (Academic, London, 1982).
[14] I. Kanter and H. Sompolinsky, Phys. Rev. Lett. **58**, 164 (1987).
[15] M. Mezard and G. Parisi, Europhys. Lett. **3**, 1067 (1987).
[16] Actually, if both spins linked by a bond have already been assigned to the same cluster, there is no need to visit the bond.
[17] M. E. Fisher, in *Critical Phenomena*, edited by M. S. Green (Academic, New York, 1972), p. 1.
[18] M. N. Barber, in *Phase Transitions and Critical Phenomena*, edited by C. Domb and J. L. Lebowitz (Academic, New York, 1983), Vol. VIII.